ELSEVIER

Materials Science and Engineering A298 (2001) 209–215

MATERIALS SCIENCE & ENGINEERING A

www.elsevier.com/locate/msea

New statistic techniques for structure evaluation of particle packing

D. He *, N.N. Ekere, L. Cai

School of Aeronautical and Mechanical Engineering, The University of Salford, Salford M5 4WT, UK

Received 10 March 2000; received in revised form 13 June 2000

Abstract

An application of statistic techniques for structure evaluation of packing of equal or distributed spherical particles is presented. The packing of particles generated by computer simulation is cut by a series of equally separated parallel planes, and the area densities of the cross-sections of particles on the cutting planes are used to analyse the packing structure. It is shown that as the number of the cutting planes increases, the mean of the area densities approaches the packing density. Then a time series analysis technique is applied to examine the randomness of the packing. The homogeneity of the packing is evaluated by testing the hypothesis that the particles are uniformly distributed within the packing space. The isotropy of the packing is evaluated both at micro-level, the distribution of projections of centre-to-centre lines between touching particles, and at macro-level, the variances of area densities on the cutting planes perpendicular to different directions. As case studies, the above techniques are applied to evaluate the packing structures of both equal and distributed particles obtained by a collective rearrangement simulation model.

Keywords: Random packing; Amorphous materials; Green compact; Structure evaluation

1. Introduction

The random packing of hard spherical particles serves as a basis for useful models of the microstructures of many materials, such as amorphous metals and semiconductors [1–3], simple liquids and glasses [4], green compacts of metallic or ceramic powders [5–7], and porous materials [8,9]. Therefore, it has been studied for many years through experiments [10–12], statistic analysis [9,13,14], and computer simulation [5–7,15–20].

The structures of crystalline materials can be represented by ordered packing of particles that exhibit periodicity and can be generated by repeating the arrangement of a small number of particles contained within a single unit cell. In contrast, the structures of amorphous materials and green compacts of powders can be represented by the random packing of particles that have to be characterised statistically. Several statistic methods have been applied to evaluate the structure of random packings, such as the packing density, coordination number, radial distribution function [1,21–23], Voronoi tessellation [1,3,18,24,25] and triangular network [3,8] statistics. The packing density is the ratio of the volume of total particles to the volume of space occupied by the particles. The coordination number is the number of particles touching a common particle. The radial distribution function is defined as [1,21]

$$\rho(R)=\frac{n(R)}{4\pi R^2\,dR} \tag{1}$$

where $n(R)$ is the mean number of particles whose distance from a given particle lie between R and $R+dR$, and dR is much smaller than the particle diameter. Thus, Eq. (1) gives the mean number of particles per unit volume at R from a given particle. The radial distribution function is an important factor for structure evaluation of particle packing. Normalising the particle diameter to one unit, Cargill [23] found that the reduced radial distribution function, $4\pi R[\rho(R)-\rho_o]$ where ρ_o is the number density of the packing, of amorphous metals was in excellent agreement with that

* Corresponding author. Tel.: +44-161-2954696; fax: +44-161-2955575.

E-mail address: d.he@salford.ac.uk (D. He).

0921-5093/01/$ - see front matter © 2001 Elsevier Science B.V. All rights reserved.
PII: S0921-5093(00)01284-3

of the random close packing of equal particles as shown in Fig. 1. It is seen that, for random close packing and amorphous metals, the value of the peaks of the radial distribution function gradually decreases with R, and approaches zero as $R>5$. In contrast, for ordered packing and crystalline metals the value of the peaks of the radial distribution function becomes significantly higher and more peaks can be observed beyond $R>5$ [3]. For packing of spherical particles, the Voronoi tessellation is derived by tracing the mediator plane between two neighbouring particles. Thus, each particle is contained by a polyhedron. The polyhedrons are classified to different types based on the edge and face numbers and the volumes. Then the packing structure can be evaluated by statistic analysis of the distribution of the polyhedron types. The triangular network is derived by tracing the centre-to-centre line between two neighbouring particles, then the centres of three neighbouring particles form a triangle. The distribution of the types of triangles, the angles and side lengths, is used to analyse the randomness at individual sub-unit level and the frequency distribution of triangle types is used at network level. Fig. 2 shows the Voronoi tessellation and the triangular network of a two-dimensional packing of discs.

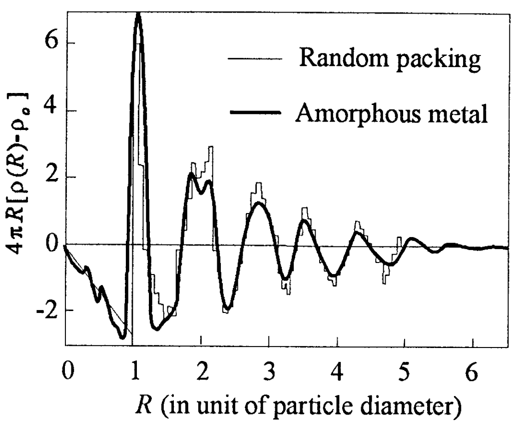

Fig. 1. Radial distribution functions of random packing and amorphous metal [23].

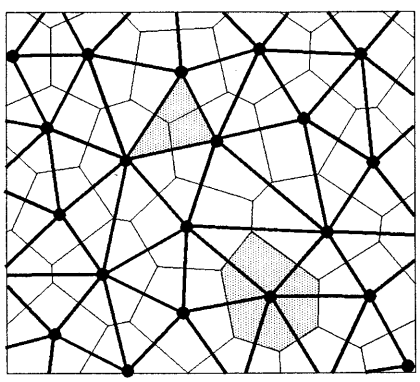

Fig. 2. Voronoi tessellations (light lines) and triangular network (heavy lines) of random packing of equal discs. The dots denote the disc centres [3].

The particle sizes of many materials, such as composites, amorphous metals and the compacts of metal or ceramic powders, are distributed [26]. The above statistic techniques are inadequate for structure evaluation of such materials. For example, the coordination number, the face number and the volume of the polyhedron of a large particle are greater than that of a small particle. We have developed new statistic techniques that are applicable to evaluate the packing structures of both equal and distributed particles. The significance of the techniques is that the three-dimensional packing is cut by a series of parallel planes and the structures of the cross-sections of particles on the planes are used to predict the three-dimensional packing structure, which leads to the simplification of analysis. In the next section we derive the statistic criteria of structure evaluation. Then as case studies, we apply the techniques to examine the packing structures of equal and distributed particles obtained by a computer simulation model. Finally we summarise the conclusion of this study.

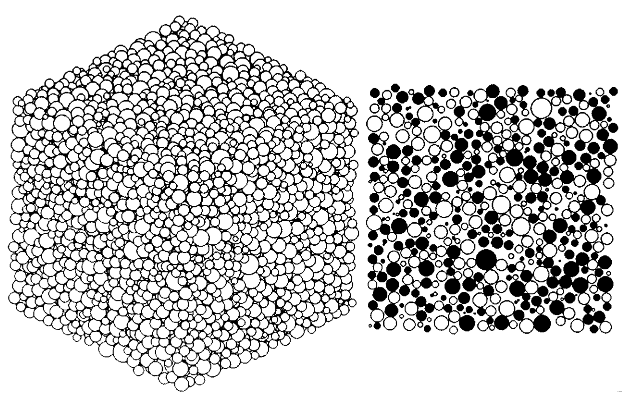

Fig. 3. Three-dimensional view of random packing and two-dimensional view on a cutting plane. The Particles with centres in front of the cutting plane are denoted by the dark circles.

2. Statistic analysis techniques

2.1. Relationship between packing density and area density on cutting plane

Fig. 3 shows the three-dimensional view of a packing of 10^4 particles within a cubic space and the two-dimensional view of the cross-sections of particles on a cutting plane. The packing density Φ is defined as

$$\Phi = \frac{4\pi}{3L^3}\sum_{i=1}^{n} r_i^3 \tag{2}$$

where n is the total number of particles, r_i is the radius of the ith particle and L is edge length of the cubic space. If the packing is cut by m equally separated

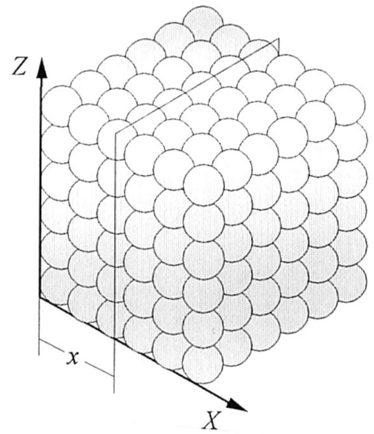

Fig. 4. Hexahedron simple cubic packing of equal particles.

parallel planes, then the area density on the jth plane is defined as

$$\Phi_{a,j}=\frac{\pi}{L^2}\sum_{k=1}^{n_j} r_k'^2 \tag{3}$$

where n_j is the number of particles cut by the jth plane and r_k' is the radius of the cross-section of the kth particle. The mean of the area densities is defined as

$$\langle\Phi_a\rangle=\frac{1}{m}\sum_{j=1}^{m}\Phi_{a,j}=\frac{\pi}{mL^2}\sum_{j=1}^{m}\sum_{k=1}^{n_j}r_k'^2=\frac{1}{L^3}\sum_{j=1}^{m}\sum_{k=1}^{n_j}\pi r_k'^2\delta l \tag{4}$$

where $\delta l=L/m$ is the distance between two adjacent planes. As m tends to infinity then Eq. (4) becomes

$$\langle\Phi_a\rangle_{m\to\infty}=\frac{1}{L^3}\int_0^L\left(\sum_{k=1}^{n_j}\pi r_k'^2\right)\mathrm{d}l=\frac{4\pi}{3L^3}\sum_{i=1}^{n}r_i^3=\Phi \tag{5}$$

Eq. (5) proves that, as m tends to infinity, the mean area density equals the packing density. Thus, the area density of the cross-sections of particles on the cutting planes can be written as

$$\Phi_{a,j}=\langle\Phi_a\rangle+\Delta\Phi_{a,j}=\Phi+\Delta\Phi_{a,j}\quad j=1,2,\ldots,m \tag{6}$$

$\Delta\Phi_{a,j}$ is the difference between $\Phi_{a,j}$ and Φ. The sum of $\Delta\Phi_a$ ($j=1, 2,\ldots, m$) equals zero and the variance of Φ_a is given by

$$S^2(\Phi_a)=\frac{1}{m-1}\sum_{j=1}^{m}\Delta\Phi_{a,j}^2 \tag{7}$$

2.2. Examination of the randomness

The structure of a crystalline material can be represented by an ordered packing of particles which exhibits periodicity. Thus, the area density Φ_a on a cutting plane is a periodical function of the position of that plane. Taking a hexahedron simple cubic packing of equal particles for example, as shown in Fig. 4, the area density on the cutting plane can be derived as

$$\Phi_a=\pi\frac{r^2-[(2j-1)r-x]}{4r^2}\quad \text{for } 2(j-1)r<x<2jr \tag{8}$$

where $j=1, 2, \ldots$, and the period of the area density is $2r$. For other ordered packings, the periodical function of the area density can also be derived. In contrast, for a random packing, the area density Φ_a must also be a random variable. We apply the time series analysis technique to evaluate the degree of randomness of the packing.

In a stochastic process, a time series is a collection of observations $\{\theta_1, \theta_2, \ldots, \theta_m\}$ of a random variable θ made sequentially over time. If the observations are taken at specific times, usually equal spaced, the time series is said to be discrete. An important guide to the properties of a time series is provided by a series of quantities, the autocorrelation coefficients, which measure the correlation between observations at different distance apart k. The autocorrelation coefficient at lag k is given by [27]

$$C_k=\frac{\sum_{j=1}^{m-k}(\theta_j-\langle\theta\rangle)(\theta_{j+k}-\langle\theta\rangle)}{\sum_{j=1}^{m}(\theta_j-\langle\theta\rangle)^2} \tag{9}$$

where $\langle\theta\rangle$ is the mean of the observations. There is often little meaningful point for $k>m/4$. We can see that $k=0$ leads to $C_k=1$. If a time series is complete randomness and the number of the observations m is sufficient large, then for all non-zero values of k, C_k approaches zero. In fact for a random time series, C_k approximately obeys normal distribution with mean value of zero and variance of $1/m$. Therefore, over 95% of the values of C_k should lie between $\pm 2/m^{1/2}$. In contrast, for different incomplete random time series the autocorrelation coefficients may show different trends of change, and for a periodic variable, it can be proved that as m tends to infinity, the autocorrelation coefficient is a periodic variable of lag k, taking $\theta=A\cos(\omega t)$ for example, the autocorrelation coefficient at lag k is given by $C_k=\cos(k\omega)$.

The above time series analysis technique can be applied to evaluate the randomness of particle packing. Instead of time spacing, we cut a packing of particles by a series of equally separated parallel planes and take the area densities on the cutting planes as the observations. Then in Eq. (9), replacing $\langle\theta\rangle$ by $\langle\Phi_a\rangle$ and θ_j by $\Phi_{a,j}$, we can obtain the autocorrelation coefficients of the area densities. If the particles are randomly packed, then from the criterion of randomness of the time series analysis, the autocorrelation coefficients of the area densities should lie between $\pm 2/m^{1/2}$, where m is the number of the cutting planes, and as m increases the autocorrelation coefficients should approach zero. For an ordered packing, such as that shown in Fig. 4 and area density given by Eq. (8), the autocorrelation coefficient is expected to be a periodic function of lag k.

2.3. Examination of homogeneity and isotropy

The structures of the random packings obtained by different computer simulation models may be either homogeneous or inhomogeneous [5,6]. For a homogeneous packing the positions of particles must obey a uniform distribution within the packing space. Therefore, we can divide the packing body into equal subregions and count the number of particles in each subregion. Then applying the χ^2 goodness-of-fit test we examine the hypothesis that the numbers of particles in the subregions obey a uniform distribution. In rigorous mathematic viewpoint, the test result either rejects or does not reject the hypothesis but it does not confirm the acceptance of the hypothesis. However, in practice the hypothesis is acceptable if it is not rejected. For unequal particles, the volume of each subregion has to be large enough to contain a reasonable number of particles to reflect the total particle size distribution. Otherwise, some subregions may be occupied by a few large particles and some by more small particles that will lead to statistic test error.

Many amorphous materials are isotropic which means the physical properties, such as the tensile stress, thermal and electrical conductivities, of such materials have no directional preference. A random packing, which is isotropic or anisotropic, can be identified by two statistic techniques. The first one is to examine the distributions of the projections of centre-to-centre lines between touching particles on the coordinate axes. With equal particles, Torry et al. [28] proved that, if the projections on any axis obey uniform distribution over (0, $2r$), the packing is isotropic. This criterion can be extended to the packings of unequal particles. We define the relative projections as

$$x'_{12} = \frac{x_{12}}{r_1 + r_2} \qquad y'_{12} = \frac{y_{12}}{r_1 + r_2} \qquad z'_{12} = \frac{z_{12}}{r_1 + r_2} \tag{10}$$

where r_1 and r_2 are the radii of two touching particles and x_{12}, y_{12} and z_{12} are the projections of the centre-to-centre line on Cartesian coordinate axes. Fig. 5 shows the relative position of two touching particles. If the packing is isotropic, then the position of particle 2 must obey uniform distribution on the spherical surface of radius $r_1 + r_2$, and the probability density function is given by $1/[4\pi(r_1 + r_2)^2]$. The probability that the projection of $r_1 + r_2$ on X-axis lies between x and $x + dx$ equals the probability that particle 2 falls on the darken section of the spherical surface, that is

$$\mathrm{d}P = \frac{\mathrm{d}A}{4\pi(r_1 + r_2)^2} = \frac{2\pi(r_1 + r_2)^2\,\mathrm{d}\alpha\,\sin\alpha}{4\pi(r_1 + r_2)^2} = \frac{\mathrm{d}\alpha\,\sin\alpha}{2} \tag{11}$$

Fig. 5 shows that $\sin\alpha = dx/[d\alpha(r_1 + r_2)]$. Then the probability density function is given by

$$f(x_{12}) = \frac{\mathrm{d}P}{\mathrm{d}x} = \frac{1}{2(r_1 + r_2)} \qquad -(r_1 + r_2) \le x_{12} < (r_1 + r_2) \tag{12}$$

Eq. (12) proves that, x_{12} obeys a uniform distribution over $\pm(r_1 + r_2)$. Replacing x_{12} by $x'_{12}\,(r_1 + r_2)$, we have density function of the relative projection, $f(x'_{12}) = 1/2$ over $(-1, 1)$, or $f(|x'_{12}|) = 1$ over (0,1). The mean and variance of $|x'_{12}|$ are 1/2 and 1/12, respectively. The relative projections are independent of the radii of the two touching particles which allows us to examine the isotropy of packing of distributed particles.

The above technique is applied to a packing at the micro-level, the relative position of touching particles. The second technique is applied at the macro-level, by which we examine the variances of the area densities on the cutting planes perpendicular to different axes. The physical meaning of this approach is easier to understand. Instead of three-dimensional random packings, which are difficult when used to observe the structural difference visually, we derive the criterion from two-dimensional ordered packings of equal discs. Then we extend the criterion to the random packing of distributed particles. Fig. 6 shows two ordered packings of equal discs. Notice that ordered packing of equal particles may represent the structures of monocrystal materials that are anisotropic. However, in Fig. 6(a), the projection of two touching discs on X equals that on Y; a material with such structure would have the same physical properties in X and Y directions. In contrast,

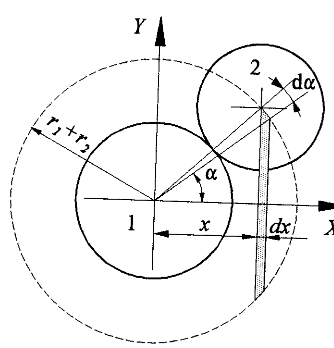

Fig. 5. The relative positions between two touching particles.

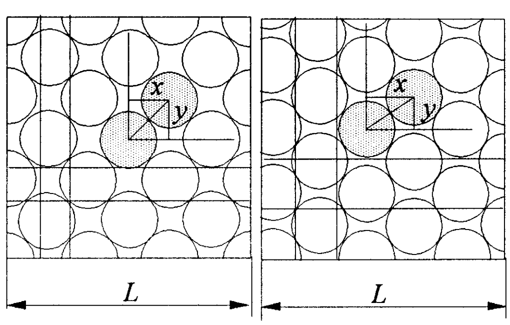

Fig. 6. Comparison of two ordered packings of equal discs.

in Fig. 6(b), the projection on X is greater than that on Y; the physical properties of a material with such structure would be different in the X direction from that in the Y direction. To identify the structural difference at macro-level, we draw m_l horizontal and m_l vertical lines on both Fig. 6(a) and Fig. 6(b). On a line we define the line density as the ratio of the sum of chords to the line length. Taking the jth line parallel to X for example, the line density is given by

$$\Phi_{lx,j} = \frac{1}{L}\sum_{k=1}^{n_j} l_k \tag{13}$$

where n_j is the number of discs cut by the jth line. Similar to Eqs. (4) and (5) we can prove that, for both structures, if m_l is sufficiently large the mean line densities, $\langle \Phi_{lx} \rangle$ and $\langle \Phi_{ly} \rangle$, both approach the area density Φ_a given by Eq. (3). The variances of Φ_{lx} and Φ_{ly} are given by

$$S^2(\Phi_{lx}) = \frac{1}{m_l}\sum_{j=1}^{m_l}(\Phi_{lx,j} - \Phi_a)^2$$

$$S^2(\Phi_{ly}) = \frac{1}{m_l}\sum_{j=1}^{m_l}(\Phi_{ly,j} - \Phi_a)^2 \tag{14}$$

In Fig. 6(a) Φ_{lx} and Φ_{ly} have the same distribution, therefore $S^2(\Phi_{lx}) = S^2(\Phi_{ly})$. In contrast, in Fig. 6(b) Φ_{lx} distributes over a broader range than Φ_{ly} does, therefore $S^2(\Phi_{lx}) > S^2(\Phi_{ly})$. This coincides with that the value of the projection on X is greater than that on Y. As stated earlier, Fig. 6(a) is anisotropic because the discs are orderly packed. The physical properties of a material with such a structure are only the same in particular directions. In fact, in Fig. 6(a), the variance of line densities in any other direction does not equal that in the X and Y directions. Therefore, from the above discussion we can infer that, a two-dimensional structure is isotropic only when the discs are randomly packed and the variances of line densities in any directions are the same. Further extending the inference to three-dimensional packing of particles, we can conclude that, a packing is isotropic only when the particles are randomly packed and the variances of area densities on the cutting planes perpendicular to any directions are the same, otherwise, the structure is anisotropic. This macro-level test criterion of the isotropic property coincides with the micro-level test criterion that the projections of centre-to-centre lines between touching particles obey uniform distribution without directional preference.

The physical meaning of the second isotropic testing method is significant. We consider a porous material that can be represented by the packing of particles. If the variances of area densities in any directions are the same, then the structure is isotropic and its resistance to liquid or gas flow will be the same in any direction. In contrast, if the variance of area densities in one direction is different from that in another direction, then the structure is anisotropic and its resistances to liquid or gas flow in the two directions will be different.

3. Case studies

We have developed a computer simulation model for random packing of particles. In this model, the particle radii and initial positions are randomly generated within a cubic space. Then the overlapped particles are gradually separated; meanwhile the packing space is expanded. The periodical boundary condition is applied to particles at the packing surface. The simulation is completed as the mean overlap value falls below $10^{-4}\langle r \rangle$, where $\langle r \rangle$ is mean of particle radii. Details of this simulation model can be found in [29]. Fig. 3 shows the three-dimensional view of a packing of 10^4 particles within a cubic space and the two-dimensional view of the cross-sections of particles on a cutting plane. The mean particle radius is normalised to one unit. The packing density of equal particles is 0.627 and the coordination number is 5.7; both agree well with the experimental results of random close packing [10]. For particles obeying log-normal distribution, with mean radius of 1.0 and standard deviation of 0.25, the packing density is 0.647 and the coordination number is 5.5. We apply the techniques developed above to examine the packing structures.

3.1. The area density and the randomness

To eliminate the boundary effect, we ignored the particles on the first surface layer, then cut each packing perpendicular to each Cartesian axis by forty equally separated planes. The area densities on the cutting planes were calculated by Eq. (3). Fig. 7(a) plots the area densities on the cutting planes perpendicular to the X direction in sequence. The horizontal lines are the packing densities. It is seen that, for both packings, the area densities are randomly distributed around the packing densities and there is no trend of periodical change. For equal particles, the mean area density is 0.628 and the standard deviation is1.18×10^{-2}. For log-normal distributed particles, the mean area density is 0.646 and the standard deviation is 7.54×10^{-3}. With 95% confidence the interval of the area density expectation is (0.624, 0.632) for equal particles, and (0.643, 0.649) for log-normal distributed particles. Both packing densities lie between the lower and upper limits of the confident intervals of the area density expectations. This supports that, as the number of cutting planes increases the mean area density approaches to the packing density.

Applying Eq. (9), the autocorrelation coefficients of area densities at lag one to lag eight ($k = 1, 2,\ldots, 8$)

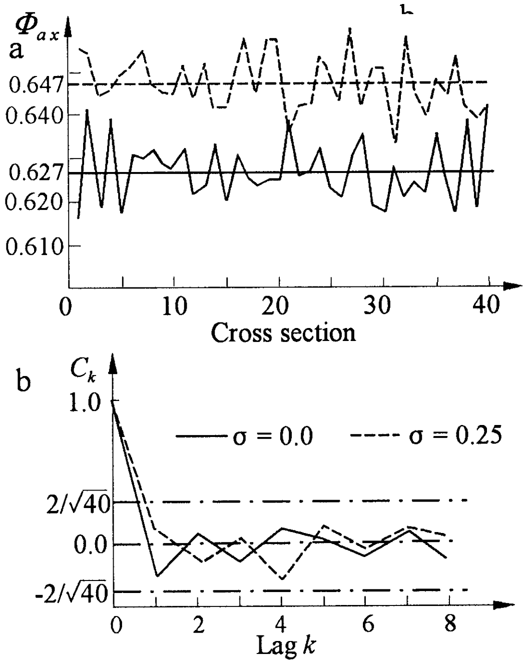

Fig. 7. Area densities on cutting planes (a) and autocorrelation coefficients (b).

Table 1
Distribution of particles among subregions

	Equal particles			Log-normal distribution $\sigma(r) = 0.25$		
Top	280	280	290	273	254	270
	283	293	284	276	271	267
	277	290	277	277	261	262
Middle	282	282	285	261	275	282
	287	286	287	270	270	259
	280	289	290	280	293	277
Bottom	289	285	272	280	281	287
	280	283	294	264	283	273
	290	284	275	280	275	260
χ^2		2.611			8.460	

were calculated as shown in Fig. 7(b). For $m = 40$, the upper and lower limits of the autocorrelation coefficients are $\pm 2/40^{1/2} = \pm 0.318$. All the autocorrelation coefficients lie between the upper and lower limits. Similar results were also obtained on the cutting planes perpendicular to the Y and Z directions. This supports that, from the criterion of randomness of time series analysis, both the equal particle packing and the log-normal distributed particle packing obtained by our simulation model are completely random. We also see that, for $k \geq 5$, the autocorrelation coefficients gradually approach zero. It is quite similar to that the peak values of the radial distribution function gradually decrease as the radial distance R increases (Fig. 1).

3.2. The homogeneous and isotropic properties of the packing

To examine the homogeneity, we divided each packing body, without considering the particles on the surface layer, into 27 equal cubic subregions and counted the number of particle centres in each cubic subregion. The results are listed in Table 1. The χ^2 goodness-of-fit test was applied to examine the hypothesis that the particles are uniformly distributed among the cubic subregions. At 0.05 level, the critical value is $\chi^2_{0.05,\ 26} = 38.885$. The test statistic for equal particles is $\chi^2 = 2.611$, and for log-normal distributed particles is $\chi^2 = 8.460$. Both test statistics are smaller than the critical value. Therefore, there is no evidence to reject the hypothesis that the particles are uniformly distributed in the packing. This implies that the packing is homogeneous. We see that the test statistic of distributed particles is greater than that of equal particles. This is because that, as stated earlier, for distributed particles some subregions contain more small particles while others contain more large particles. We found that, in the subregions containing fewer particles, the mean particle diameter is statistically larger than that containing more particles.

The isotropy of the packing was tested by both methods. By the first method, we examined the relative projection distributions on X-, Y- and Z-axes. Table 2 gives the means and variances of the projections, and Fig. 8 shows the distribution of the projections on X-axis. We accepted that, by hypothetical test, the relative projections on X-, Y- and Z-axes obey uniform distributions over (0, 1). By the second method, we examine the variances of area densities on the cutting planes perpendicular to different axes. For equal particles, the sample variances of area densities on the cutting planes perpendicular to X-, Y- and Z-axes are $S^2(\Phi_{ax}) = 1.392 \times 10^{-4}$, $S^2(\Phi_{ay}) = 1.854 \times 10^{-4}$ and $S^2(\Phi_{az}) = 1.537 \times 10^{-4}$ respectively. From statistic theory, the ratios $F_{xy} = S^2(\Phi_{ax})/S^2(\Phi_{ay})$ and $F_{yz} = S^2(\Phi_{ay})/S^2(\Phi_{az})$ obey F distribution. The hypotheses are $\sigma^2(\Phi_{ax}) = \sigma^2(\Phi_{ay})$ and $\sigma^2(\Phi_{ay}) = \sigma^2(\Phi_{az})$, where σ^2 is

Table 2
The means and variances of projections

	Mean (x') S^2 (x')	Mean (y') S^2 (y')	Mean (z') S^2 (z')
Equal particles	0.4986	0.5012	0.4999
	0.0832	0.0832	0.0828
Log-normal distribution $\sigma(r) = 0.25$	0.4998	0.5005	0.5002
	0.0832	0.0832	0.0828

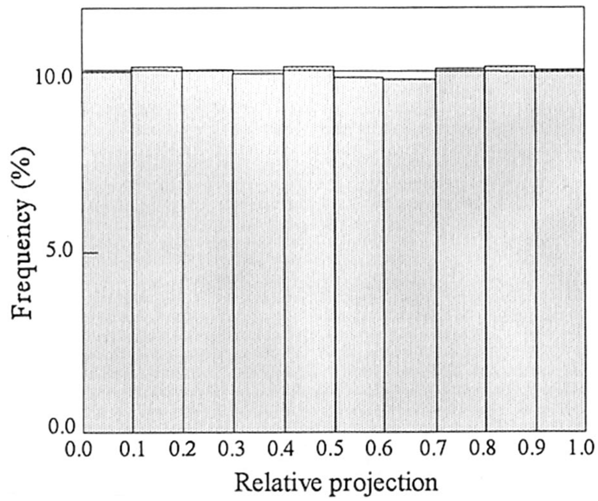

Fig. 8. Distribution of projections on X-axis.

the variance as m tends to infinity. At 0.05 level, the lower and upper tails of F distribution are $F(40,40)_{0.025}=0.533$ and $F(40,40)_{0.975}=1.88$. The test statistics are $F_{xy}=0.751$ and $F_{yz}=1.206$, both lie between the lower and upper tails. This suggests us to accept the hypotheses. For distributed particles, the variances of the area densities are $S^2(\Phi_{ax})=0.568\times 10^{-4}$, $S^2(\Phi_{ay})=0.556\times 10^{-4}$ and $S^2(\Phi_{az})=0.426\times 10^{-4}$. Similar hypothetical tests showed no significant difference between the variances. The results of the hypothetical tests are consistent with that the projections of touching particles on X-, Y- and Z-axes obey uniform distributions over (0, 1). Both micro-level and macro-level tests suggest that the packings generated by our simulation model are isotropic. Different simulation models may generate different structures. For random packing generated by sequential central growing model [5,6], the packing density decreases in the radial direction so the structure is inhomogeneous. For random packing generated by gravitational model [28], the mean projection on Z-axis is greater than that on X- and Y-axes so the structure is anisotropic.

4. Conclusion

New statistic techniques for structure evaluation of particle packing have been developed. The advantages of the techniques are that the area densities on the cutting planes are used to predict the structure properties which provides physical significance, and the techniques are applicable to the packing of distributed particles. By statistic analysis we have proved that: (1) as the number of cutting planes m increases, the mean area density approaches the packing density; (2) if the values of the autocorrelation coefficients of area densities, C_k ($k=1$, 2...), lie between $\pm 2/m^{1/2}$, then the packing is completely random; (3) dividing the packing into equal subregions, if the particles are uniformly distributed among the subregions, then the packing is homogeneous; and (4) if the projections of centre-to-centre lines between touching particles on any axis obey uniform distribution over (0, 1), or if the variance of the area densities on the cutting planes perpendicular to any axis is statistically the same, then the packing is isotropic.

As case studies, we have applied the above techniques to examine the structures of packings of equal and distributed spherical particles obtained by a collective rearrangement simulation model, and results showed that the packings are completely random, homogeneous and isotropic.

Acknowledgements

This research was funded by the Engineering and Physical Sciences Research Council of the United Kingdom under Grant No. GR/L20597.

References

[1] J.L. Finney, Mater. Sci. Eng. 23 (1976) 199.
[2] G.S. Cargill, J. Appl. Phys. 41 (1970) 12.
[3] R. Zallen, The Physics of Amorphous Solids, Wiley, New York, 1998, pp. 33–85.
[4] G.Y. Onoda, E.G. Liniger, Phys. Rev. Lett. 64 (1990) 2727.
[5] Y. Konakawa, K. Ishizaki, Powder Technol. 63 (1990) 241.
[6] G.Q. Lu, X. Shi, J. Mater. Sci. Lett. 13 (1994) 1709.
[7] D. He, N.N. Ekere, J. Mater. Sci. Lett. 17 (1998) 1723.
[8] Z.P. Zhang, A.B. Yu, R.B.S. Oakeshott, J. Phys. A Math. Gen. 29 (1996) 2671.
[9] Y. Rouault, S. Assouline, Powder Technol. 96 (1998) 33.
[10] G.D. Scott, Nature 188 (1960) 908.
[11] J.D. Bernal, J. Mason, Nature 188 (1990) 910.
[12] H.Y. Sohn, C. Moreland, Can. J. Chem. Eng. 46 (1968) 162.
[13] K. Gotoh, J.L. Finney, Nature 252 (1974) 202.
[14] J.G. Berryman, Phys. Rev. A 27 (1983) 1053.
[15] W.M. Visschor, M. Bolsterli, Nature 239 (1972) 504.
[16] C.H. Bennett, J. Appl. Phys. 43 (1972) 2727.
[17] W.S. Jodrey, E.M. Tory, Phys. Rev. A 32 (1985) 2347.
[18] A.S. Clarke, J.D. Wiley, Phys. Rev. B 35 (1987) 7350.
[19] G.T. Nolan, P.E. Kavanagh, Powder Technol. 76 (1993) 309.
[20] A. Yang, G.T. Miller, L.D. Turcoliver, Phys. Rev. E 53 (1996) 1516.
[21] G.D. Scott, Nature 194 (1962) 956.
[22] G. Mason, Nature 217 (1968) 733.
[23] G.S. Cargill, Solid State Phys. 30 (1975) 227.
[24] A. Gervois, J.P. Troadec, J. Lemaitre, J. Phys. A Math. Gen. 25 (1992) 6169.
[25] J. Lemaitre, A. Gervois, J.P. Troadec, N. Rivier, M. Ammi, L. Oger, D. Bideau, Phil. Mag. B 67 (1993) 347.
[26] H. Rumpf, Particle Technology, Chapman and Hall, London, 1990, pp. 20–28.
[27] C. Chatfield, The Analysis of Time Series An Introduction, Chapman and Hall, London, 1989, pp. 18–23.
[28] E.M. Tory, B.H. Church, M.K. Tam, M. Ratner, Can. J. Chem. Eng. 51 (1973) 484.
[29] D. He, N.N. Ekere, L. Cai, Phys. Rev. E 60 (1999) 7098.